

## Electrochemical Properties of Hybrid Supercapacitors Formed Based on Carbon and ABO<sub>3</sub>-Type Perovskite Materials

H.M. Kolkovska<sup>1</sup>, I.P. Yaremiy<sup>1</sup>, P.I. Kolkovskyi<sup>1,2</sup>, S-V.S. Sklepova<sup>1</sup>, B.I. Rachiy<sup>1</sup>,  
A.G. Belous<sup>2</sup>, M.O. Halushchak<sup>3</sup>

<sup>1</sup> *Vasyl Stefanyk Precarpathian National University, 57, Shevchenko St., 76018 Ivano-Frankivsk, Ukraine*

<sup>2</sup> *Vernadsky Institute General and Inorganic Chemistry, Kiev, Ukraine*

<sup>3</sup> *Ivano-Frankivsk National Technical University of Oil and Gas, Ivano-Frankivsk, Ukraine*

(Received 14 January 2021; revised manuscript received 20 February 2022; published online 28 February 2022)

In this work, lanthanum (LaMnO<sub>3</sub>), strontium (SrMnO<sub>3</sub>) and Sr-doped lanthanum (La<sub>0.7</sub>Sr<sub>0.3</sub>MnO<sub>3</sub>) manganites with the perovskite structure were synthesized by the sol-gel autocombustion method. Moreover, the obtained material structure was investigated by the XRD method. Additionally, the electrochemical properties of nanoporous carbon materials (CMs), lanthanum (LaMnO<sub>3</sub>) and strontium (SrMnO<sub>3</sub>) manganites, as well as La<sub>0.7</sub>Sr<sub>0.3</sub>MnO<sub>3</sub> were investigated by the methods of chronoamperometry and voltammetry, and the application of these materials as electrodes (anode and cathode) of hybrid electrochemical supercapacitors (HECs) was tested. The hybrid electrochemical system of the CM/KOH/La<sub>0.7</sub>Sr<sub>0.3</sub>MnO<sub>3</sub> type was formed. The employment of this system made it possible to increase the operating voltage range of HEC based on aqueous electrolytes from 0-1 to 0-1.4 V and, consequently, increase the energy characteristics of a unit cell. It was determined that high specific capacitance values were recorded for HECs with an electrode based on La<sub>0.7</sub>Sr<sub>0.3</sub>MnO<sub>3</sub> and amounted to about 235 F/g at 1 mV/s. At the same time, much lower specific capacitance values were obtained for HECs with electrodes based on LaMnO<sub>3</sub> and SrMnO<sub>3</sub>, which were about 130 F/g and 40 F/g, respectively.

**Keywords:** Electrochemical energy storage devices, Lanthanum manganites, Porous carbon material, Aqueous electrolyte.

DOI: [10.21272/jnep.14\(1\).01020](https://doi.org/10.21272/jnep.14(1).01020)

PACS numbers: 81.07.Wx, 82.45.Yz, 82.47.Uv

### 1. INTRODUCTION

Electrochemical capacitors (ECs) are one of the most common devices for storing electricity due to their high values of specific power, long cycle time, and short charge/discharge time [1, 2]. Carbon materials (CMs) of various modifications are the most common materials for the manufacture of EC electrodes [3, 4]. The main advantages of CMs are low cost, ease of production and versatility of existing forms (foam, powders, nanotubes, composites, monoliths, foil). ECs with electrodes based on CMs with a large surface area work on the principle of charge/discharge of the electric double layer (EDL) [5, 6]. The amount of charge accumulated in the EDL is not large enough, despite the large specific surface area of CM, which in turn limits the specific capacity and energy density of the device. Therefore, one of the ways to increase the energy density of ECs is the formation of hybrid EC (HECs), in which positive and negative electrodes are formed based on materials with different mechanisms of electric charge accumulation, namely EDL and Faraday process, thus expanding the operating voltage range [7, 8]. Furthermore, the Faraday process is carried out due to the reversible redox reaction on the electrode surface [9]. The electrode materials for the Faraday process are transition metal oxides (for example, RuO<sub>2</sub>, MnO<sub>2</sub>, NiO, Co<sub>2</sub>O<sub>3</sub>, etc.) and leading polymers (for example, polyaniline, polypyrrol, etc.) [10-16]. The perovskite materials of the ABO<sub>3</sub> type are of great research interest among metal oxides due to their excellent electronic structure, good thermal stability, and exceptional ionic conductivity. Moreover, lanthanum manganites with the perovskite structure are attracting much attention due to their promising electri-

cal properties. The authors of [17] suggested that the electrical properties of lanthanum manganites with the perovskite structure correspond to the interaction between Mn<sup>3+</sup> and Mn<sup>4+</sup> ions. The control of Mn<sup>3+</sup> and Mn<sup>4+</sup> ions in the material structure is provided by changing the doping level or oxygen stoichiometry [18]. Therefore, by combining CMs with perovskite structures, it is possible to obtain hybrid electrode materials for supercapacitors characterized by low cost, high electrical conductivity and chemical stability. In order to solve the problem of low values of specific energy, specific power and operation time of conventional supercapacitors, in this work, we studied the effect of the porous structure of CMs on the electrochemical characteristics of HECs formed based on lanthanum (LaMnO<sub>3</sub>) and strontium (SrMnO<sub>3</sub>) manganites and Sr-doped LaMnO<sub>3</sub> (La<sub>0.7</sub>Sr<sub>0.3</sub>MnO<sub>3</sub>) with the perovskite structure.

### 2. EXPERIMENTAL TECHNIQUE

#### 2.1 Synthesis of LaMnO<sub>3</sub>

Lanthanum manganite LaMnO<sub>3</sub> (LMO) with the perovskite structure was synthesized by the sol-gel method involving autocombustion, the procedure of which is described in detail in [18]. For the synthesis of complex oxide SrMnO<sub>3</sub> (SMO), the sol-gel method with the participation of autocombustion was also used. However, for the synthesis of LMO, 0.01 M lanthanum nitrate (La(NO<sub>3</sub>)<sub>3</sub>×6H<sub>2</sub>O), 0.01 M manganese nitrate (Mn(NO<sub>3</sub>)<sub>2</sub>×6H<sub>2</sub>O) and 0.02 M citric acid (C<sub>6</sub>H<sub>8</sub>O<sub>7</sub>×H<sub>2</sub>O) were dissolved in deionized solution. To establish the pH level = 7, a small amount of 25 % aqueous ammonia solution was added to the resulting solution, until ob-

taining a milky pink solution. After continuous stirring the solution for 4 h, a maroon (purple) solution was obtained. The resulting sol was placed in a furnace at 120 °C for 10-12 h until completely dry. A polycondensation reaction occurred between citric acid and metal nitrates to form a gel during the dehydration process. Then the resulting material was heated to 300 °C. A few minutes later, autocombustion of the xerogel occurred, as a result of which a free-flowing LaMnO<sub>3</sub> product was obtained. A similar synthesis method was used to obtain Sr-doped LaMnO<sub>3</sub> complex oxide (La<sub>0.7</sub>Sr<sub>0.3</sub>MnO<sub>3</sub>) with the perovskite structure.

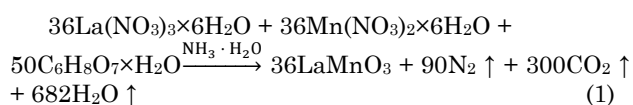
## 2.2 Research Methods

The crystal structure of the sample was determined by X-ray diffraction (XRD) using a Shimadzu XRD-7000 diffractometer. The results of the obtained diffractograms were subjected to a full-profile analysis according to the Rietveld method using the FullProf program. The size of nanocrystallites of the research sample and its phase composition were determined from the analysis of X-ray structural data.

Electrochemical studies of the electrode material/electrolyte system were performed in a three-electrode cell. The working electrode was made of a mechanical mixture of the test material and acetylene carbon black in a ratio of 85:10:5. A platinum electrode served as an auxiliary electrode, and silver chloride (Ag/AgCl) served as a reference electrode, which was placed in a 3.5 M aqueous KCl solution and connected to the working chamber through an agar-agar salt bridge. A 30 % aqueous solution of KOH was used as an electrolyte. Electrochemical studies were carried out using an Autolab PGSTAT/FRA-2 spectrometer in galvanostatic and potentiodynamic modes. The galvanostatic investigation was performed at currents in a range of 1 to 30 mA. Cyclic voltammetry investigations were carried out at a scan rate of 1 to 30 mV/s. The operational characteristics of laboratory samples of ECs were determined in a two-electrode cell. In HECs, the cathode was made from a mechanical mixture of ABO<sub>3</sub>, acetylene black and PVDF in a ratio of 85:10:5. Another electrode (anode) was made by mixing CM with acetylene black and PVDF in a ratio of 85:10:5. Finally, the resulting electrode materials were pressed into a nickel grid. The electrodes were impregnated with the electrolyte, separated by a separator, and placed in a two-electrode cell of the 25×25 size, after which they were sealed.

## 3. RESULTS AND DISCUSSION

The LaMnO<sub>3</sub> compound is formed as a result of a chemical reaction:



The technology and features of the synthesis of the studied material are described in [19]. The crystal structure of SrMnO<sub>3</sub> and La<sub>0.7</sub>Sr<sub>0.3</sub>MnO<sub>3</sub> (LSMO) was investigated using XRD analysis (CuK<sub>α</sub> radiation) in an angle range of 10° < 2θ < 70°.

Fig. 1a shows the diffraction patterns of LSMO. From the experimental XRD patterns, it was found that the diffraction peak (2θ = 23, 32, 40, 46, 52, 58, 68) for the obtained material is well indexed with the La<sub>0.7</sub>Sr<sub>0.3</sub>MnO<sub>3</sub> cubic phase.

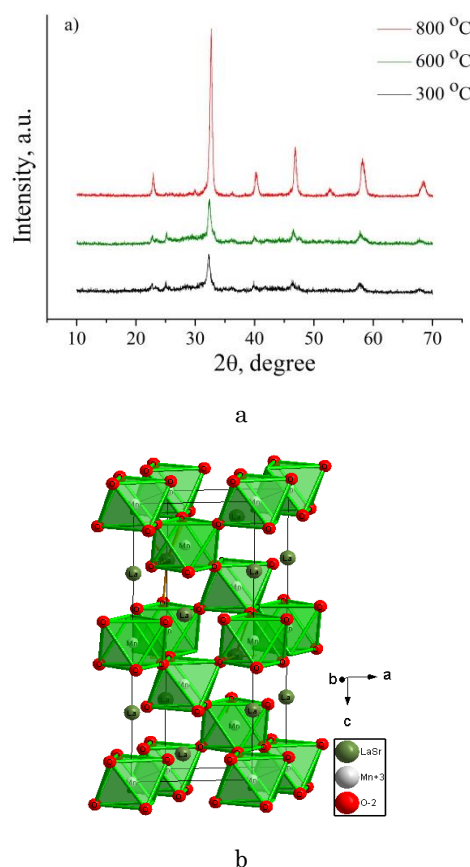


**Fig. 1** – XRD patterns of the synthesized LSMO at an annealing temperature of 300, 600 and 800 °C (a) and a model of the LSMO crystal structure (b-axis view) (b)

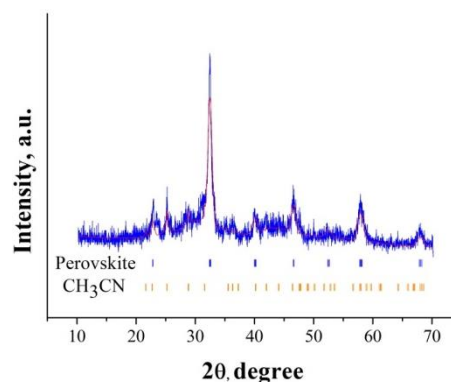


**Fig. 2** – XRD pattern of the synthesized La<sub>0.7</sub>Sr<sub>0.3</sub>MnO<sub>3</sub> at an annealing temperature of 300 °C

However, the obtained material is not single-phase and contains both the expected La<sub>0.7</sub>Sr<sub>0.3</sub>MnO<sub>3</sub> phase and an organic chemical compound such as acetonitrile CH<sub>3</sub>CN (Fig. 2). The presence of an organic compound indicates that not all organic substances from the xerogel components burned out during the autocombustion reaction. Sintering at 600 °C for 3 h was used to remove the organic compound (Fig. 3).

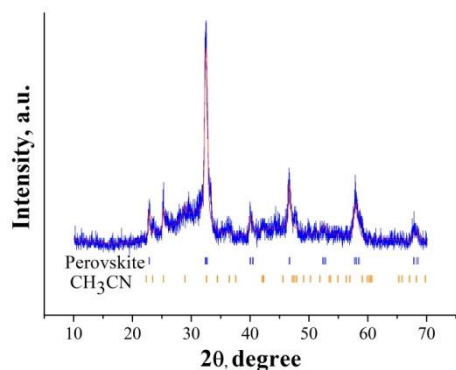


**Fig. 3** – XRD pattern of the synthesized  $\text{La}_{0.7}\text{Sr}_{0.3}\text{MnO}_3$  at an annealing temperature of 600 °C

XRD analysis of the sample after sintering showed that the amount of the organic compound in the sample decreased, but the sample remained two-phase. To obtain a single-phase system, another annealing was carried out at a temperature of 800 °C (Fig. 4a). As a result of this annealing, a single-phase material  $\text{La}_{0.7}\text{Sr}_{0.3}\text{MnO}_3$  was obtained. The FullProf program was used to calculate the theoretical diffraction pattern using the Rietveld method for a more detailed analysis of X-ray structural data. Details and features of using this program are described in [20].

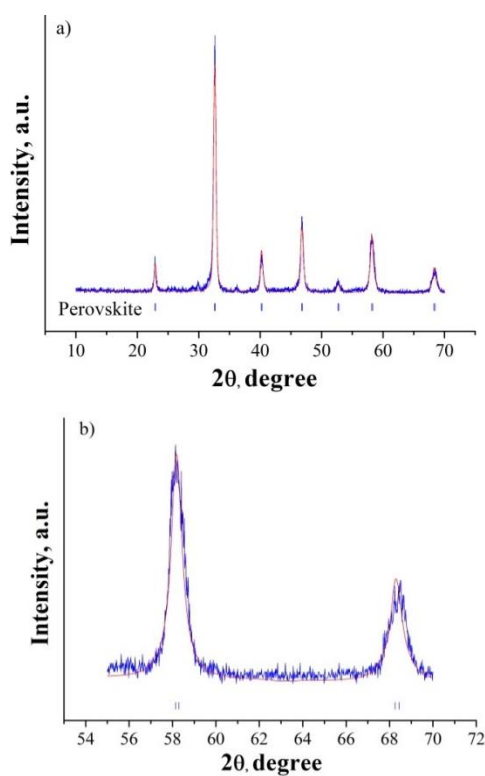


**Fig. 4** – XRD pattern of the synthesized  $\text{La}_{0.7}\text{Sr}_{0.3}\text{MnO}_3$  at an annealing temperature of 800 °C (cubic lattice with space group Pm-3m was used for fitting)

In general, the undistorted perovskite structure has a cubic lattice with a Pm-3m space group. The crystal lattice is distorted due to the large ionic radius of the cations included in the structure of the studied perovskite, which leads to a decrease in the symmetry of the

crystal structure and manifests itself in XRD patterns in the splitting of peaks characteristic of the cubic structure and the appearance of new peaks. Symmetry reduction in perovskite leads to the formation of an orthorhombic structure or a trigonal structure. In our case, the appearance of new peaks compared to the cubic structure is not observed. Therefore, the obtained perovskite is not characterized by an orthorhombic structure possible for this type of compounds (P2c2ab). The use of the Rietveld method made it possible to refine the structure of the synthesized perovskite. According to the refined data (Fig. 5a), the resulting  $\text{La}_{0.7}\text{Sr}_{0.3}\text{MnO}_3$  belongs to a trigonal system with space symmetry group R3m (160).

Consideration of cubic and trigonal structures when interpreting the diffractograms confirmed that the synthesized material has a trigonal structure R3m, which is clearly seen from a comparison of Fig. 4b and Fig. 5b, where the decoupling of lines at large angles clearly shows that each experimental reflection consists of several lines (Fig. 5a).

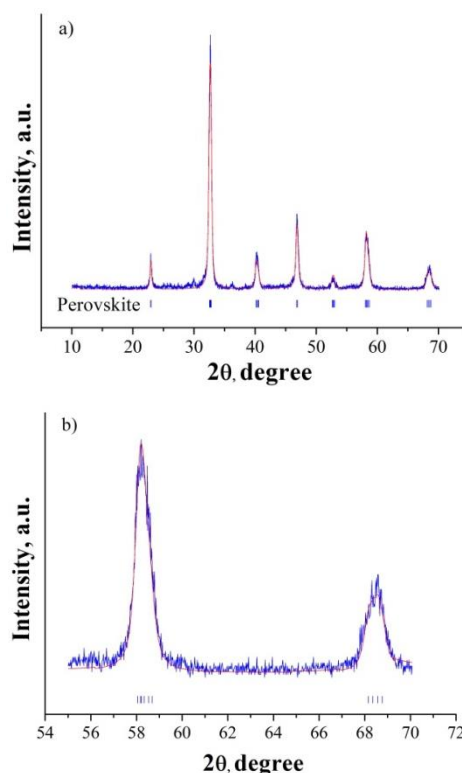


**Fig. 5** – XRD pattern of the synthesized  $\text{La}_{0.7}\text{Sr}_{0.3}\text{MnO}_3$  at an annealing temperature of 800 °C (trigonal structure R3m was used for fitting)

Furthermore, this result is consistent with the results obtained in [21]. The parameters of the perovskite crystal lattice, within the accuracy of their determination, decrease with increasing annealing temperature (Fig. 5b), which is explained by the healing of defects in the crystal structure when the material is held at high temperatures [22, 23].

The average sizes of CSR blocks, which were determined according to [24], increased during the annealing from 300 to 600 °C. Moreover, annealing at 800 °C had little effect on their sizes.

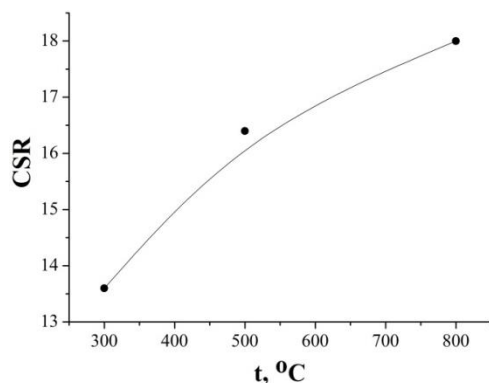


**Fig. 6** – Dependence of the CSR parameters of the crystal lattice of the perovskite structure on temperature

The structure and behavior of the  $\text{SrMnO}_3$  sample upon annealing were similar. Thus, materials obtained after annealing at 800 °C were used as materials for supercapacitors for further research.

Potentiodynamic studies of ECs with electrodes based on  $\text{SrMnO}_3$ ,  $\text{LaMnO}_3$  and  $\text{La}_{0.7}\text{Sr}_{0.3}\text{MnO}_3$  nanosized materials were carried out in 1 M KOH aqueous solution in a potential window from  $-0.23$  to 1 V relative to the (Ag/AgCl) electrode at different scan rates from 1 mV/s. Fig. 7b shows comparative CVA curves of ECs with electrodes based on  $\text{SrMnO}_3$ ,  $\text{LaMnO}_3$  and  $\text{La}_{0.7}\text{Sr}_{0.3}\text{MnO}_3$  nanosized materials at a scan rate of 10 mV/s. Moreover, CVA curves of ECs with electrodes based on  $\text{La}_{0.7}\text{Sr}_{0.3}\text{MnO}_3$  nanosized material at different scan rates from 1 to 30 mV/s are shown in Fig. 7a. Furthermore, Fig. 7a shows that for all CVA curves, there is a deviation from a rectangular shape, which indicates interruptions in the redox reaction both on the charge and discharge branches.

High specific capacitance values were recorded for EC with an electrode based on  $\text{La}_{0.7}\text{Sr}_{0.3}\text{MnO}_3$  and amounted to about 235 F/g at 1 mV/s. At the same time, slightly lower specific capacitance values were obtained for ECs with electrodes based on  $\text{LaMnO}_3$  and  $\text{SrMnO}_3$ , which were about 130 F/g and 40 F/g, respectively (Fig. 7c), which can probably be associated with the structural and morphological features of the materials under study. At low scan rates, electrolyte ions, namely OH-hydroxyl groups, get enough time to interact and electrochemically react with electrochemically active centers, which leads to an increase in specific capacitance.

The CV curves of  $\text{La}_{0.7}\text{Sr}_{0.3}\text{MnO}_3$  have a redox peak at about 0.8 V (against the Ag/AgCl electrode), which corresponds to the  $\text{Mn}^{3+} \leftrightarrow \text{Mn}^{4+}$  transition [25]. The charge imbalance arising in the crystal lattice of  $\text{LaMnO}_3$  due to the replacement of  $\text{La}^{3+}$  ions by  $\text{Sr}^{2+}$  ions is compensated either by the oxidation of  $\text{Mn}^{3+}$  ions to  $\text{Mn}^{4+}$  or by the introduction of oxygen vacancies.

The main role in charge accumulation is played by the intercalation of ions with active centers in both alkaline and neutral electrolytes. Fig. 8 shows the voltammograms obtained for the CM/KOH/ $\text{La}_{0.7}\text{Sr}_{0.3}\text{MnO}_3$  system at various operating potentials and a scan rate of 1 mV/s. Moreover, the operation of the electrochemical system is stable over the entire voltage range.

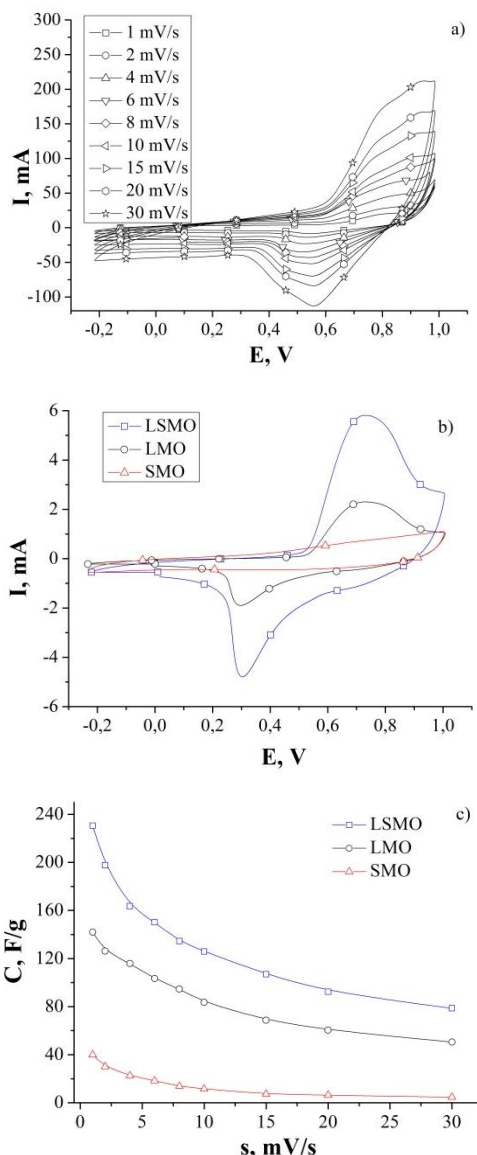


**Fig. 7** – Potentiodynamic curves for the LSMO/electrolyte system, at scan rates from 1 to 30 mV/s (a), the same for the SMO, LMO and LSMO systems at 10 mV/s (b) and specific capacitance values of the corresponding systems (c)

Based on the experimentally obtained potentiodynamic curves (Fig. 8a), the specific capacitances of the CM/KOH/ $\text{La}_{0.7}\text{Sr}_{0.3}\text{MnO}_3$  system were determined as follows: 27.0, 39.3 and 46.7 F/g according to the values of the working potential of 0-1, 0-1.2 and 0-1.4 V, respectively. The model of the CM/KOH/ $\text{La}_{0.7}\text{Sr}_{0.3}\text{MnO}_3$  system showed stability in the voltage range of 0-1.4 V (Fig. 8b). Therefore, further electrochemical studies were performed in this potential range (Fig. 9a).

The CV curves for the  $\text{La}_{0.7}\text{Sr}_{0.3}\text{MnO}_3$ /electrolyte/CM system have a redox peak of about 0.9 V (against the CM electrode), which corresponds to the  $\text{Mn}^{3+} \leftrightarrow \text{Mn}^{4+}$  transition. The maximum value of specific capacitance for the  $\text{La}_{0.7}\text{Sr}_{0.3}\text{MnO}_3$ /electrolyte/CM system was obtained at a scan rate of 1 mV/s and is about 210 F/g with a gradual decrease to about 60 F/g with an increase in the scan rate up to 30 mV/s (Fig. 9b).

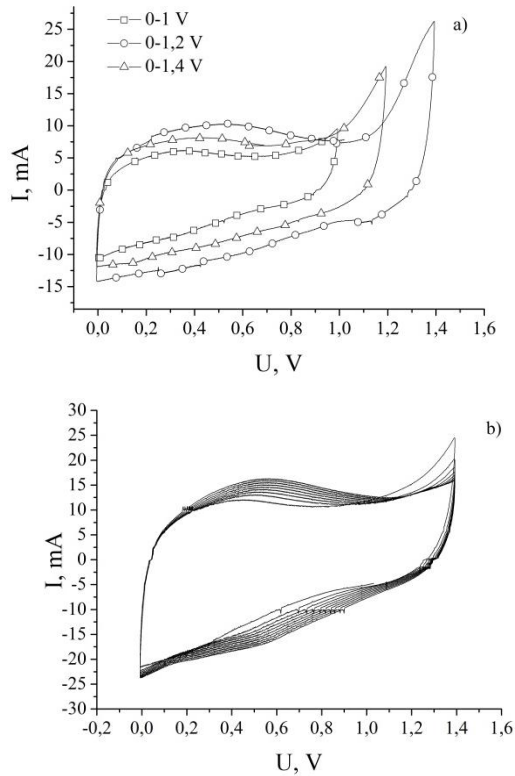


**Fig. 8** – CVA curves of the CM/KOH/La<sub>0.7</sub>Sr<sub>0.3</sub>MnO<sub>3</sub> system at different operating potentials (a), stability cycling of the CM/KOH/La<sub>0.7</sub>Sr<sub>0.3</sub>MnO<sub>3</sub> system in the voltage range of 0-1.4 V (b)

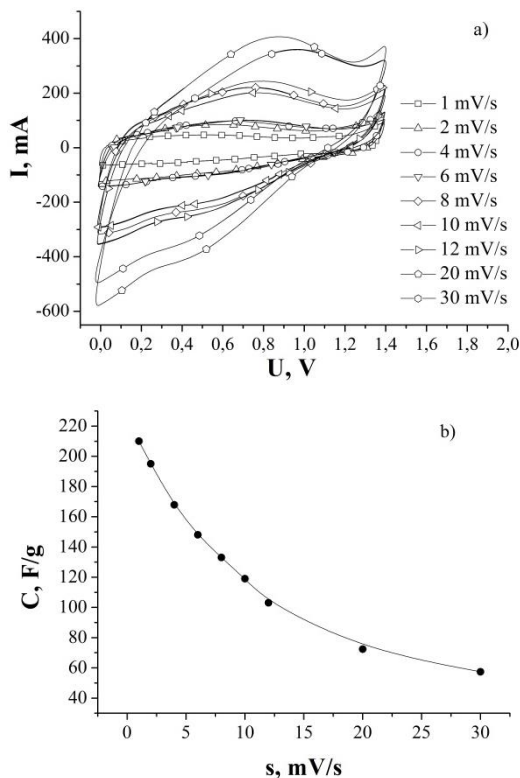


**Fig. 9** – Potentiodynamic curves of La<sub>0.7</sub>Sr<sub>0.3</sub>MnO<sub>3</sub>/electrolyte/CM at scan rates of 1-30 mV/s (a) and dependence of capacitance on scan rate (b)

Fig. 10a shows the charge/discharge curves for the La<sub>0.7</sub>Sr<sub>0.3</sub>MnO<sub>3</sub>/electrolyte/CM system obtained by the

galvanostatic method from 0 to 1.4 V, corresponding to the capacitance of the EDL formed at the electrode/electrolyte interface and pseudo-capacitance due to charge accumulation. Using the experimentally obtained discharge curves (Fig. 10a), the dependence of the specific capacitance of the system on the value of the discharge current was calculated (Fig. 10b). The value of the specific capacitance at a discharge current of 1 mA is 205 F/g and gradually decreases with increasing discharge current.

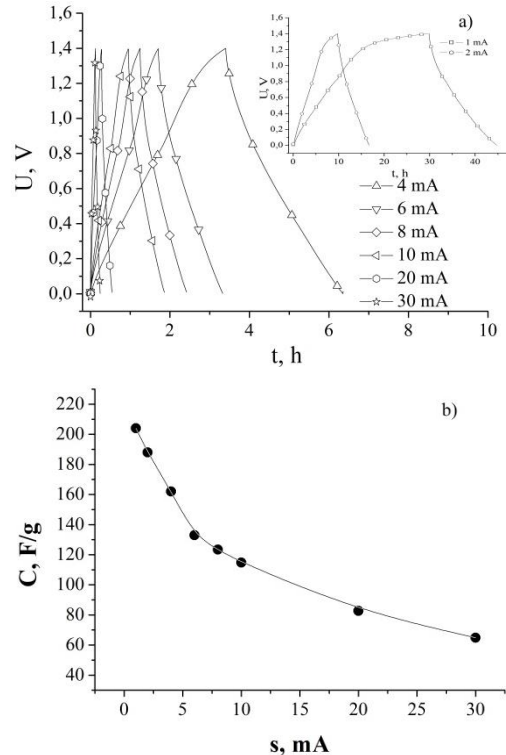


**Fig. 10** – Galvanostatic curves (a) at different charge/discharge currents (1-30 mA); dependence of capacitance of La<sub>0.7</sub>Sr<sub>0.3</sub>MnO<sub>3</sub>/electrolyte/CM on discharge current (b)

#### 4. CONCLUSIONS

A method has been proposed for obtaining modified LaMnO<sub>3</sub> with the perovskite structure doped with Sr as an electrode material for hybrid electrochemical systems with high energy and capacitance characteristics. The possibility of operation of a hybrid electrochemical system based on nanoporous carbon and perovskite materials of the ABO<sub>3</sub> type in an alkaline electrolyte has been shown. It has been established that La<sub>0.7</sub>Sr<sub>0.3</sub>MnO<sub>3</sub> can be successfully used as an anode material for HECs with high specific energy at an operating voltage of the element for aqueous electrolytes of 1.4 V. Moreover, anodes based on La<sub>0.7</sub>Sr<sub>0.3</sub>MnO<sub>3</sub> have higher specific capacitance than HECs, in which LaMnO<sub>3</sub> and SrMnO<sub>3</sub> are used as anodes. It has been determined that the maximum specific capacitance of 205 F/g at an operating current of 1 mA is exhibited by HECs, in which La<sub>0.7</sub>Sr<sub>0.3</sub>MnO<sub>3</sub> was used as an anode. It has been shown that in HECs based on CMs and La<sub>0.7</sub>Sr<sub>0.3</sub>MnO<sub>3</sub> it is possible to increase the operating voltage to the limits of 1-1.4 V, which provides, accordingly, their highest energy characteristics.

## REFERENCES

1. F. Wang, X. Wu, X. Yuan, Z. Liu, Y. Zhang, L. Fu, Y. Zhu, Q. Zhou, Y. Wu, W. Huang, *Chem. Soc. Rev.* **46**, 6816 (2017).
2. C. Largeot, C. Portet, J. Chmiola, P. Taberna, Y. Gogotsi and P. Simon, *J. Am. Chem. Soc.* **130**, 2730 (2008).
3. R.Y. Shvets, I.I. Grygorchak, A.K. Borysyuk, S.G. Shvachko, A.I. Kondyr, V.I. Baluk, A.S. Kurepa, and B.I. Rachiy, *Phys. Solid State* **56**, 2021 (2014).
4. B.K. Ostafiychuk, I.M. Budzulyak, M.M. Kuzyshyn, B.I. Rachiy, R.A. Zatorskiy, R.P. Lisovski, V.I. Mandzyuk, *J. Nano-Electron. Phys.* **5**, 03049 (2013).
5. B.E. Conway, *Electrochemical Supercapacitors- Scientific Fundamentals and Technological Applications* (New York: Kluwer Academic. Plenum: 1999).
6. E. Frackowiak, F. Beguin, *Carbon* **39**, 937 (2001).
7. V. Khomenko, E. Raymundo-Pinero, E. Frackowiak, F. Beguin, *Appl. Phys. A* **82**, 567 (2005).
8. J.P. Zheng, *J. Electrochem. Soc.* **150**, A484 (2003).
9. M. Salanne, B. Rotenberg, K. Naoi, K. Kaneko, P.L. Taberna, C.P. Grey, B. Dunn, P. Simon, *Nat. Energy* **1**, 16070 (2016).
10. H. Xia, Y. Shirley Meng, G. Yuan, C. Cui, L. Lu, *Electrochem Solid St.* **15**, A60 (2012).
11. A. Ray, A. Roy, S. Saha, M.Ghosh, S. Roy Chowdhury, T. Maiyalagan, S. Kumar Bhattacharya, S. Das, *Langmuir*, **35**, 8257 (2019).
12. P.I. Kolkovskiy, B.K. Ostafiychuk, M. I. Kolkovskiy, N. Y. Ivanichok, S.S. Sklepova, B.I. Rachiy, *Phys. Chem. Solid State* **21**, 621 (2020).
13. A. Roy, A. Ray, P. Sadhukhan, S. Saha, S. Das, *Mater. Res. Bull.* **107**, 379 (2018).
14. H. Zhu, J. Liu, Q. Zhang, J. Wei, *Int. J. Energy Res.* **44**, 8654 (2020).
15. Chodankar, Nilesh R., Rama Raju, G. Seeta, Park, Bumjun, Shinde, Pragati A., Chan Jun, Seong, Dubal, Deepak P., Huh, Yun Suk, Han, *J. Mater. Chem. A* **8**, 5721 (2020).
16. N.R. Chodankar, S.J. Patil, Rama Raju, D. W. Lee, Deepak P. Dubal, Y. S. Huh, Y.-K. Han, *Chem. Sus. Chem.* **13**, 1582 (2020).
17. P.G. Gennes, *Phys. Rev.* **118**, 141 (1960).
18. H.M. Kolkovska, B.I. Rachiy, P.I. Kolkovskiy, I.P. Yaremiy, N.Ya. Ivanichok, R.P. Lisovski, N.R. Ilytskyi, *Phys. Chem. Solid State* **22**, 644 (2021).
19. B.K. Ostafiychuk, H.M. Kolkovska, I.P. Yaremiy, B.I. Rachiy, P.I. Kolkovskiy, N.Y. Ivanichok, S.I. Yaremiy, *Phys. Chem. Solid State* **21**, 219 (2020).
20. I. Yaremiy, S. Yaremiy, V. Fedoriv, O. Vlasii, A. Lucas, *J. Enterprise Technol.* **5**, 61 (2018).
21. A. G. Belous, O.I. V'yunov, E.V. Pashkova, O.Z. Yanchevskii, A.I. Tovstolytkin, A.M. Pogorelyi, *Solid Solutions. Inorganic Mater.* **39**, 161 (2003).
22. I.V. Horichok, L.I. Nykyruy, T.O. Parashchuk, S.D. Bardashevska, M.P. Pylyponuk, *Mod. Phys. Lett. B* **1**, 1650172 (2016).
23. I.V. Gorichok, P.M. Fochuk, Ye.V. Verzhak, T.O. Parashchuk, D.M. Freik, O.E. Panchuk, A.E. Bolotnikov, R. B.James. *J. Cryst. Growth* **415**, 146 (2015).
24. В.С. Бушкова, С.І. Мудрий, І.П. Яремій, В.І. Кравець, *Журнал фізичних досліджень* **20** № ½, 1702 (2016.)
25. Y. Cao, B. Lin, Y. Sun, H. Yang, X. Zhang, *J. Alloys Compd.* **638**, 204 (2015).

### Електрохімічні властивості гібридних суперконденсаторів, сформованих на основі вуглецю та перовскітних матеріалів типу АВО<sub>3</sub>

Г.М. Колковська<sup>1</sup>, І.П. Яремій<sup>1</sup>, П.І. Колковський<sup>1,2</sup>, С.-В.С. Склепова<sup>1</sup>, Б.І. Рачій<sup>1</sup>,  
А.Г. Білоус<sup>2</sup>, М.О. Галушак<sup>3</sup>

<sup>1</sup> Прикарпатський національний університет імені Василя Стефаника, Івано-Франківськ, Україна

<sup>2</sup> Інститут загальної та неорганічної хімії імені Вернадського, Київ, Україна

<sup>3</sup> Івано-Франківський національний технічний університет нафти і газу, Івано-Франківськ, Україна

В роботі синтезовано манганіти лантану (LaMnO<sub>3</sub>), стронцію (SrMnO<sub>3</sub>) та LaMnO<sub>3</sub>, допованого Sr, (La<sub>0.7</sub>Sr<sub>0.3</sub>MnO<sub>3</sub>) зі структурою перовскіту методом золь-гель автогоріння. Досліджено структуру отриманих матеріалів методом XRD, методами хроноамперометрії та вольтамперометрії вивчено електрохімічні властивості нанопористих вуглецевих матеріалів (ВМ), манганітів лантану, стронцію, а також La<sub>0.7</sub>Sr<sub>0.3</sub>MnO<sub>3</sub>, і досліджено застосування цих матеріалів як електродів гібридних електрохімічних конденсаторів (ГЕК). Сформовано гібридну електрохімічну систему типу ВМ/КОН/La<sub>0.7</sub>Sr<sub>0.3</sub>MnO<sub>3</sub>. Використання такої системи дозволяє підвищити робочий діапазон напруги ГЕК на основі водних електродитів з 0-1 до 0-1,4 В, а отже, підвищити енергетичні характеристики елемента. Встановлено, що високі значення питомої ємності отримано для ГЕК з електродом на основі La<sub>0.7</sub>Sr<sub>0.3</sub>MnO<sub>3</sub>, що становить близько 235 Ф/г при 1 мВ/с. У той же час для ГЕК з електродами на основі LaMnO<sub>3</sub> та SrMnO<sub>3</sub> отримано дещо нижчі значення питомої ємності, які становлять близько 130 Ф/г і 40 Ф/г відповідно.

**Ключові слова:** Електрохімічне накопичення енергії, Манганіти лантану, Гібридні суперконденсатори, Пористий вуглецевий матеріал, Водний електродит.